



DISCOVERY

(International Multidisciplinary Refereed Research Journal)

(Peer-reviewed, Refereed, Indexed & Open Access Journal)

ISSN:

DOI:

IMPACT FACTOR:

Effects of Powder Bed Temperature on Ti-6Al-4V Alloy Fabricated via Selective Laser Melting

Sachin SHISHODIA¹, Kamal Kishor SHARMA², Zakir ALI³

^{1,2,3}Department of Mechanical Engineering
IIMT College of Polytechnic, Greater Noida

¹Sachin3897_gn@iimtindia.in, ²kamalkishorsharma2312_gn@iimtindia.in

DOI No:

DOI Link:

ABSTRACT

The use of laser powder bed fusion (LPBF) in the precise production of complex formed structure parts is growing need of the industry. During production, the martensitic microstructure of the Ti-6Al-4V alloy is easily formed. Preheating the powder bed can improve the mechanical characteristics by enhancing the thermal field created by cyclic laser heating during LPBF. All of the Ti-6Al-4V alloy samples produced by LPBF in the present research exhibit a near-full densification state, with a densification ratio of above 99.4%. The specimens are made of a single type of α -martensite when the temperature of the powder bed is less than 400 °C. As the temperature rises over 400 °C, the V element diffuses and redistributes, that leads to precipitate at the limits of the α -martensite. Additionally, as the temperature of the powder bed rises, the α/α lath becomes coarser. The specimens created at temperatures below 400 °C have a high strength but poor ductility. Additionally, when the temperature rises above 400 °C, the ultimate tensile strength and yield strength somewhat decline while the ductility increases significantly.

Keywords: Powder, Bed, Laser, Temperature, Beam, Power, Layer, Fusion

1.0 INTRODUCTION

In SLM, a platform is covered in a thin layer of metal powder, which is then fused selectively in an inert gas environment using a powerful laser beam. When the first layer has been scanned, the main platform is lowered by the thickness of the subsequent layer, and powder is once more dispersed on a platform using a roller. This process is repeated until the last layer has been applied [4-6]. Biomedical components and aeronautical spare parts are frequently created using SLM since it is quicker and allows for the creation of complicated parts with superior mechanical qualities, especially high specific strength of the part. Laser power, laser spot, number of heat sources, laser beam wavelength, scan velocity, working volume, layer thickness, material used, build envelope capacity, and inert gas consumption are the most crucial process parameters for PBF printers [6, 7]. A PBF machine's main characteristic is its laser power, which can be anywhere between 100 and 1000 watts [8]. Laser spot sizes range from 50 to 500 μ m. Almost all SLM printers use a Nd:YAG and fibre laser with a wavelength of 1060 nm. In a PBF machine, the scan velocity is a variable parameter that may be selected by the user in order to obtain precise results for the part. Depending on the size of the part to be manufactured, the working volume is dependent on the chamber volume. The variable parameter of layer thickness ranges from 20 to 200 μ m. the variety of materials that can be processed in accordance with needs. Build envelope capacity, which typically ranges from 5 to 50 cm³/h, is inversely connected to resolution of accuracy and directly proportional to scan velocity. In SLM machines, the printing process is carried out in a secluded chamber that is typically filled with Argon, an inert gas. Between 30 and 300 l/h of gas are consumed [8–10]. According to Figure 1.1, a generic powder bed fusion printer has the following chambers: a build platform chamber and scanning system, where the final object is constructed using a high-energy laser; a powder supply and recoating system, which aids in spreading metal powder via a recoater blade. Figure 1.2 shows the working principle of laser melting under powder bed fusion and solidification phenomenon in selective laser melting.

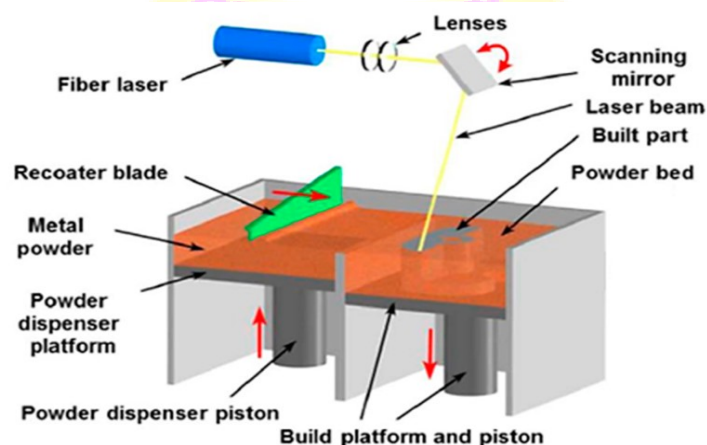


Figure 1.1: Components of generic Powder bed Fusion Printer [9].

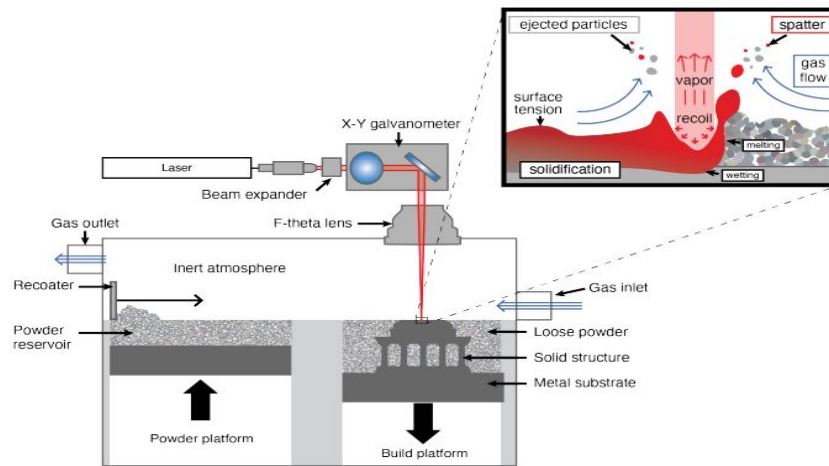


Figure 1.2: Working principle of Selective laser melting under PBF [13]

2.0 Materials and Methods

2.1 Experimental design and analysis

Processing parameters used are the laser power (P) of 200 W and the scanning speed (v) of 1000 mm/s. The powder layer thickness (t) of 30 μm and a stripe filling strategy with the hatch distance (h) of 150 μm were applied. The laser energy density (E) was 45 J/mm³, and this value was obtained using the following equation: $E = P/(vth)$ as shown in Fig.2.1, then using Netfabb simulation utility to perform analysis which helps to obtain the results of displacement and stress distribution as shown in Fig.2.2 and Fig.2.3 respectively.

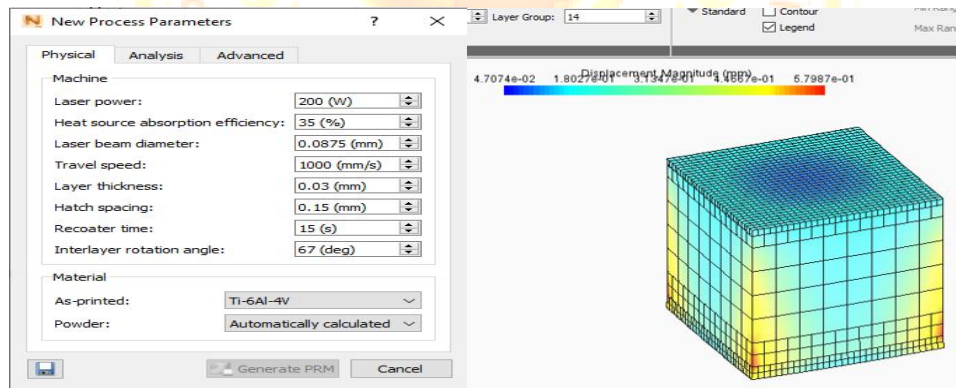


Figure 2.1: Process Parameters to create PRM file Figure 2.2: Displacement magnitude

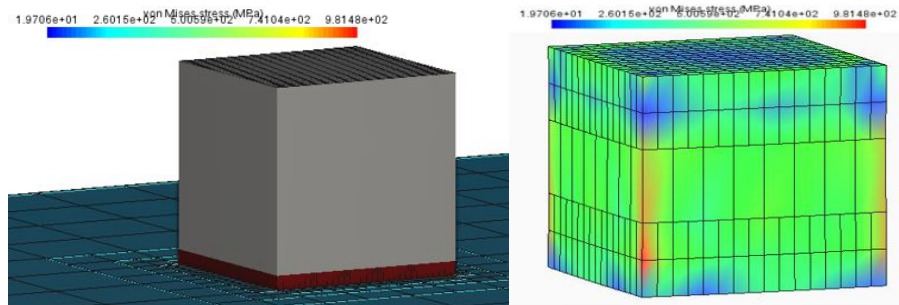


Figure 2.3 Stress distribution

Table 2.1: Results obtained

Properties	Values
Maximum stress	981 MPa
Maximum displacement	0.57 mm

3D model (Cubic bar of 10*10*10mm³) is created using creo-parametric as shown in Fig.2.4(a) and Stereo lithography (stl) file is saved, this. stl file is then imported in Autodesk Netfabb as shown in Fig.2.4(b). A machine of SLM solutions 280HL 1.0 is added from the added machine list in Autodesk Netfabb 2021. This machine is equipped with a fiber modulated pulse laser with a maximum power of 800 W and wavelength of 1070 nm.

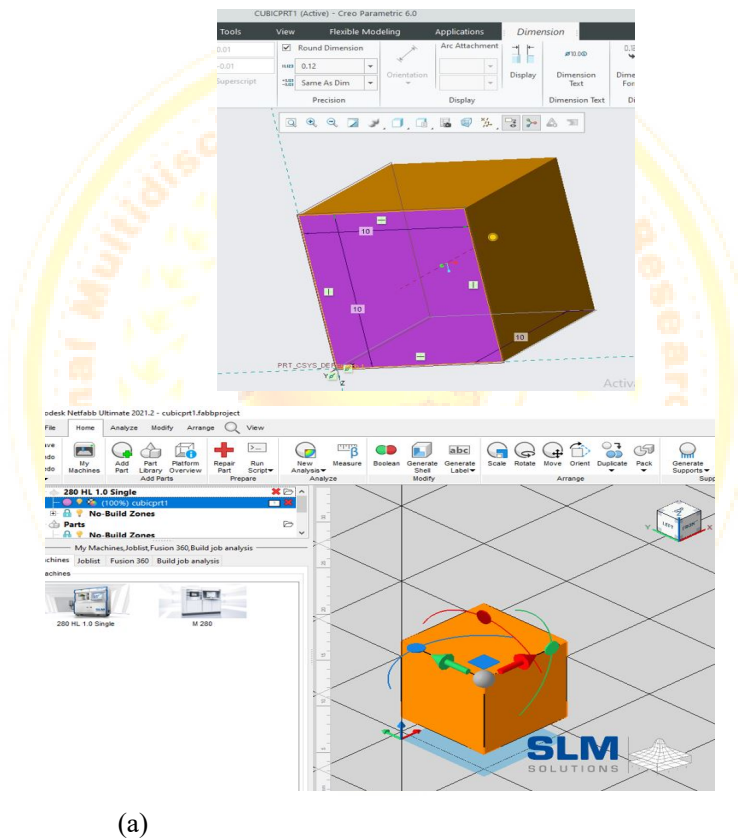


Figure 2.4: (a) 3D Model (b) Stl file imported in Netfabb

Now process parameters such as material Ti-6Al-4V, Machine configurations and supports are selected as shown in Fig.2.5(a). The build chamber was filled with argon gas to maintain an inert atmosphere as shown in Fig.2.5(b). A multi-directional meander scan strategy was used where the laser scan direction was rotated by 67° for each layer to reduce residual stresses. Fig.2.5(c) shows that component was built on a Ti-6Al-4V metal substrate preheated to 60 °C. The temperature of the build chamber during the process was 34-36 °C.

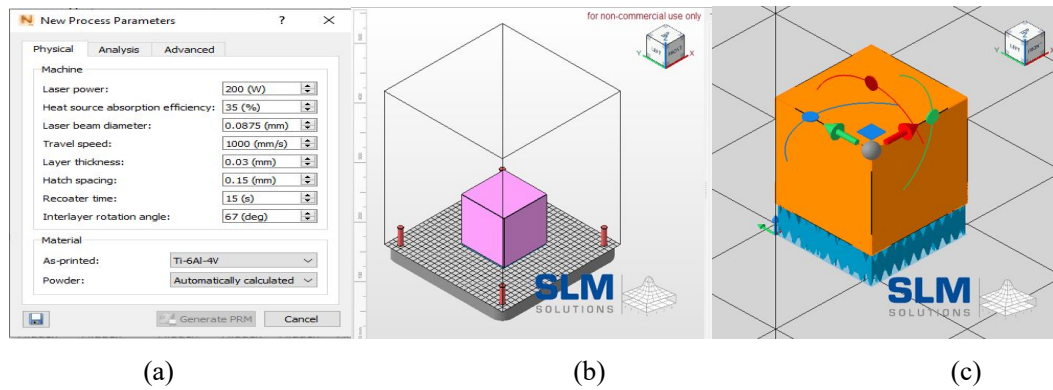


Figure 2.5: (a) Machine configurations & parameters selection (b) SLM 280HL1.0 build chamber (c) build support

Thermal analysis of Multiple-cube specimens with a dimension of 10 mm × 10 mm × 10 mm were performed using Autodesk Netfabb at various temperatures as unheated, 200 °C, 400 °C and 600 °C. Keeping Constant Processing parameters as shown in Table 2.2 below. Figure 2.6(a) shows the window to enter build plate/bed temperature.

Table 2.2: Thermal analysis Parameters under SLM at different bed temperatures

Bed Temp.	Laser Power(W)	Scanning Speed (mm/s)	Powder Layer Thickness(μm)	Hatch Distance(μm)	Energy Density (J/mm ³)
Unheated	200	1000	30	150	45
200 °C					
300 °C					
400 °C					
500 °C					
600 °C					

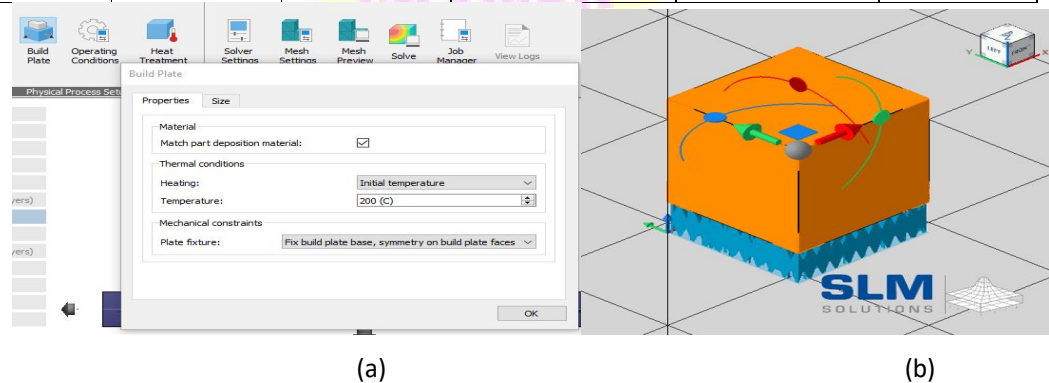


Figure 2.6: (a) Entering build plate/bed temperature (b) build plate/bed shown below supports

Fig.2.7 shows the stress distribution at different bed temperatures, which depicts that maximum stress is obtained at unheated bed condition which shows the unheated powder bed shows highest

strength and worst ductility. As the powder bed temperature increases, the tensile performance exhibits a trade-off phenomenon in strength and ductility; specifically, the ultimate tensile and yield strengths decrease, whereas ductility improves.

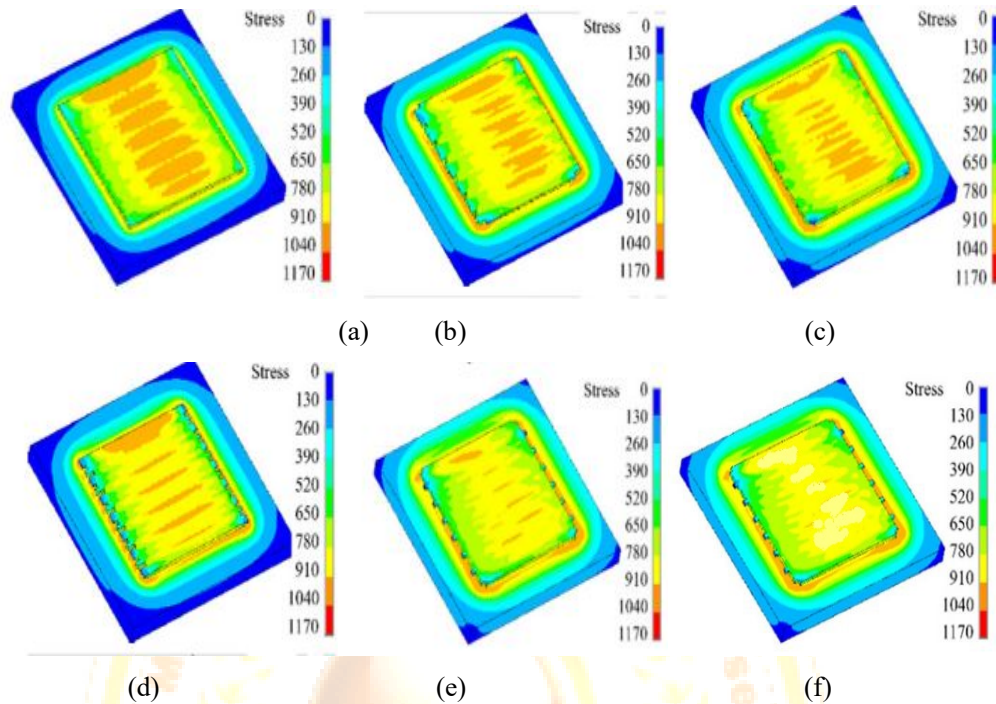


Figure 2.7: Stress distribution at (a) unheated bed (b) 200 °C (c) 300°C (d) 400 °C (e) 500°C (f) 600°C

Stress-strain curve is generated using MATLAB, as we have ultimate stress which is higher in unheated powder bed condition and minimum in case of 600°C as shown in Fig.2.8(a) below and Fig.2.8(b) shows the yield and ultimate strength at different powder bed conditions.

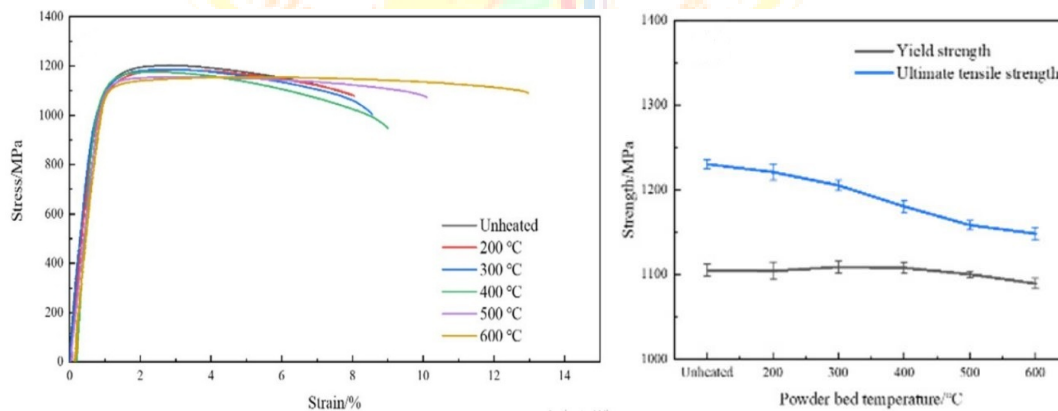


Figure 2.8: (a) Stress strain curve at different bed temperature (b) Strengths

Conclusion

The specimens manufactured at the temperature lower than 400 °C exhibit high strength but bad ductility. Moreover, the ultimate tensile strength and yield strength reduce slightly, whereas the ductility is improved dramatically with the increasing temperature, when it is higher than 400 °C.

References

1. Kruth, G.; Levy, F.; Klocke and T. Childs.; Consolidation phenomena in laser and powder bed based layered manufacturing. *CIRPAnnals*. **2007**, 56(2), 730- 759.
<https://doi.org/10.1016/j.cirp.2007.10.004>
2. Mueller Bernhard.; Additive manufacturing technologies - Rapid prototyping to direct digital manufacturing, *Assembly Automation 2012*, 32(2).
<https://doi.org/10.1108/aa.2012.03332baa.010>
3. Liu, S.; Shin, Y.; Additive Manufacturing of Ti6Al4V alloy: A review, *Materials and Design* **2019**, 164, 107552 , <https://doi.org/10.1016/j.matdes.2018.107552>
4. Ishwer, S.; Golam, K.; Soham, D.; Ashis S.; Bal Bahadur Pradhan & Chatterjee, s.; Laser surface texturing on Ti-6Al-4V, *Materials and Manufacturing Processes* 2021, 36(7), 858-867, <https://doi.org/10.1080/10426914.2020.1866197>
5. Prisco, U.; Astarita, A.; El Hassanin & Franchitti, S.; Influence of processing parameters on microstructure and roughness of electron beam melted Ti-6Al-4V titanium alloy, *Materials and Manufacturing Processes*2019, 34(15), 1753-1760, <https://doi.org/10.1080/10426914.2019.1683576>
6. S.P.Leo ; Avinash , D.; Review on effect of Ti-alloy processing techniques on surface- Integrity for biomedical application, *Materials and manufacturing processes* **2020**, 35(8), 69-892. <https://doi.org/10.1080/10426914.2020.1748195>
7. Shipley, H.; McDonnell, D.; Culleton, M.; Coull, R.; Lupoi, R.; O'Donnell ; Trimble, D.; Optimisation of process parameters to address fundamental challenges during selective Laser melting of Ti-6Al-4V: A review, *International Journal of Machine Tools and Manufacture***2018**, 128, 1-20, <https://doi.org/10.1016/j.ijmachtools.2018.01.003>
8. Kaschel, F. R.; Celikin,M.; Dowling, D.P.; Effects of laser power on geometry, Microstructure and mechanical properties of printed Ti-6Al-4V parts, *Journal of Materials Processing Technology* **2020**, 278, 116539,
<https://doi.org/10.1016/j.jmatprotec.2019.116539>
9. Criaes, L.E.; Arisoy, Y.M.; Lane, B.; Moylan, S.; Donmez, A.; Özel, T.. Laser powder Bed fusion of nickel alloy625: Experimental investigations of effects of process parameters on melt pool size and shape with spatter analysis.*Int. J. Mach. Tool Manuf.* **2017**, 121, 22–36.<https://doi.org/10.1016/j.ijmachtools.2017.03.004>
10. Tan,C.; Zhou,K.; Ma,W.; Attard,B.; Zhang, P.; Kuang,T.; Selective laser melting of high-Performance pure tungsten: parameter design, densification behavior and mechanical properties, *Science and Technology of Advanced Materials*, **2018**, 19(1), 370-380,
<https://doi.org/10.1080/14686996.2018.1455154>

11. Thijs, L.; Frederik, V.; Tom C.; Humbeeck, J.; Kruth, J. Study of the microstructure evolution during selective laser melting of Ti-6Al-4V. *Acta Materialia* **2010**, 58(9), 3303-3312. <https://doi.org/10.1016/j.actamat.2010.02.004>
12. Vrancken, L.; Thij, J.; Kruth and J. Van Humbeeck.; Heat treatment of Ti6Al4v produced by Selective Laser Melting: Microstructure and mechanical properties. *Journal of Alloys and Compounds*. **2012**, 541, 177- 185. <https://doi.org/10.1016/j.jallcom.2012.07.022>
13. Lie, C.; Tsai,T.; Tseng, C.; Numerical simulation of heat and mass transfer during selective laser melting of titanium alloys powder .*Physics Procedia*. **2016**, 83, 1444-1449. <https://doi.org/10.1016/j.phpro.2016.08.150>
14. Chen, Q.; Guillemot,G.; Gandin, C.G.; Bellet, M.; Three-dimensional finite element thermo mechanical modeling of additive manufacturing by selective laser melting for ceramic materials, *Addit. Manuf.* **2017**, <https://doi.org/10.1016/j.addma.2017.02.005>
15. Paolo, C. P.; Vincenzo, L.; Eleonora, A.; Alessandro, S.; Laser powder bed fusion (L-PBF) additive manufacturing: On the correlation between design choices and process sustainability, *Procedia CIRP*, **2018**, 78, 85-90 , <https://doi.org/10.1016/j.procir.2018.09.058>
16. Xiacong He; Finite Element Analysis of Laser Welding: A State of Art Review, *Materials and Manufacturing Processes* **2012**, 27(12) , 1354-1365, <https://doi.org/10.1080/10426914.2012.709345>
17. Peter, N.; Pitts, Z.; Thompson, S.; Saharan, A.; Benchmarking build simulation software for LPBF of metals, *Additive Manuf.* **2020**, 36, 12-20. <https://doi.org/10.1016/j.addma.2020.101531>
18. Murr, L.; Quinones, S.; Gaytan, S.; Microstructure and mechanical behavior of Ti-6Al-4V produced by rapid-layer manufacturing for biomedical applications, *Journal of the Mechanical Behavior of Biomedical Materials*.**2009**, 2(1), 20-32. <https://doi.org/10.1016/j.jmbbm.2008.05.004>
19. Shunmugavel, M.; Polishetty, A.; Littlefair, G.; Microstructure and mechanical properties of wrought and additive manufactured Ti-6Al-4V cylindrical bars, *Procedia Technology*. **2015**, 20, 231-236.<https://doi.org/10.1016/j.protec.2015.07.037>
20. Vaithilingam, J.; Prina,E.; Ruth,G.; Richard, J.M.; Steve,E.; Felicity, R.; Steven ,D.R. C.; Surface chemistry of Ti6Al4V components fabricated using selective laser melting for biomedical applications, *Materials Science and Engineering C*, **2016**, 67, 294-303. <https://doi.org/10.1016/j.msec.2016.05.054>
21. Xuanyong, L.; Paul, K.C.; Chuanxian, D.; Surface modification of titanium, titanium alloys, and related materials for biomedical applications, *Materials Science and Engineering: R: Reports*, **2004**, 47(3-4), 49-121. <https://doi.org/10.1016/j.msere.2004.11.001>

22. Zhou X, Liu X, Zhang D, et al. Balling phenomena in selective laser melted tungsten. *J Mater Process Technol.* **2015**, 222, 33–42.
23. Sibisi, P.N., Popoola, A.P.I., Arthur, N.K.K. et al. Review on direct metal laser deposition manufacturing technology for the Ti-6Al-4V alloy. *Int J Adv Manuf Technol*, **2020**, 107, 1163–1178 <https://doi.org/10.1007/s00170-019-04851-3>
24. Ducato, Antonino & Fratini, Livan & La Cascia, Marco & Mazzola, Giuseppe. An Automated Visual Inspection System for the Classification of the Phases of Ti-6Al-4V Titanium Alloy, *Computer Analysis of Images and Patterns conf.*, **2013**, 362-369. https://doi.org/10.1007/978-3-642-40246-3_45
25. Xing, L.-L.; Zhang, W.-J.; Zhao, C.-C.; Gao, W.-Q.; Shen, Z.-J.; Liu, W. Influence of Powder Bed Temperature on the Microstructure and Mechanical Properties of Ti-6Al-4V Alloys Fabricated via Laser Powder Bed Fusion. *Materials*, *MDPI*, 2021, 14, 2278. <https://doi.org/10.3390/ma14092278>

